

# Control Modeling and Fault Simulation Analysis in Microgrid

Jiang Li ,Xu Yanlu, Zhu Heyan, Zhang Mingli, Yu Changyong,  
Lu Tianqi

*State Grid Liaoning Electric Power CO,LTD. Power Electric Research Institute, Shenyang, Liaoning110015, China*

**ABSTRACT.** *The microgrid contains a large number of inverter based distributed generators, whose operation control and fault characteristics are different from that of traditional synchronous generators. The inverter control mode is analyzed. The simulation model of different operation control modes (grid-connected operation and islanding operation) in the microgrid is established on the DlgSILENT simulation software. The fault characteristics of both side and distribution line side, and the influence of the fault protection under different operation control modes are analyzed and compared, which provides the basis for the protection strategy of the distributed power microgrid.*

**KEYWORDS:** *inverter modeling; islanding operation; fault simulation*

## 1. Introduction

With the improvement of power electronics technology and automatic control technology, as well as people's awareness of environmental protection, distributed power generators (DGs) using renewable energy are increasingly connected to the distribution network. In general, the distributed power supply in the distribution network exists near the load. Currently, most of the small-capacity distributed power supplies are Inverter Based Distributed Generators (IBDGs). The IBDG is installed on each feeder of the distribution network, which is close to the user, and its transmission loss is small. The provision of active power and the compensation of reactive power are also more rapid and convenient, and the access of the distributed power supply makes the distribution network Power supply reliability and power quality have been improved [1-3].

However, the access of a large number of IBDGs poses a problem for distribution network protection. The single-ended power radiating distribution system becomes a multi-terminal power supply system, and the direction of the power flow in the distribution network changes intermittently. Existing distribution system protection devices need to be adjusted to accommodate the uncertainty of the

direction of the flow [4-5]. The IBDG is integrated into the grid from the DC through the inverter, and the voltage, current and frequency output on the AC side are determined by the control mode of the inverter [6-7]. In different control modes, the scale and characteristics of faults are also very different.

At present, the research on the fault characteristics of IBDG mostly focuses on the grid-connected control (PQ control) mode, and lacks the fault simulation of IBDG as the main FM power supply under the island operation [8-9]. When the IBDG is in island operation, the inverter uses constant voltage constant frequency control (V/f control) to ensure the balance of power and voltage and frequency stability in the island [10-11]. Therefore, the short-circuit capacity of the microgrid in grid-connected operation and island operation is very different. The IBDG under different control also has different output characteristics. It is necessary to fully consider the impact of the inverter on the existing protection under different control strategies.

In the existing literature, the fault simulation of IBDG mostly analyzes the output response change on the power supply side, and there is little fault analysis on the line side. However, the literature on transient analysis of line side faults generally does not establish a simulation model for IBDG alone, and more is simplified by ordinary power supply [12-13].

Based on DIgSILENT software, this paper establishes a simulation control model for IBDG under different control modes (PQ control, V/f control), and performs fault simulation for the microgrid in the running state of grid connection and island. Not only on the power supply side, the fault characteristics of the IBDG in two modes of operation are analyzed; the effects of IBDG on the transient currents at both ends of the line (such as current phase and amplitude variation) are also summarized, which is a multi-IBDG microgrid system. The protection strategy provides a theoretical basis.

## **2. IBDG modeling based on DIgSILENT**

### ***2.1 Double loop current control***

In this paper, IBDG's inverter control is based on rotating coordinate double loop current control (as shown in Figure 1).

Through the Park transformation, the AC variation of the stationary coordinate system acquired on the grid side can be converted into the DC variation in the rotating coordinate system. The current actual control amount of the power outer loop is obtained by the power calculation module. Under the dq rotation coordinate, the expressions of the active power P and the reactive power Q are as shown in (1). The PLL (Phase Lock Loop) module tracks the net side phase angle  $\theta$  by collecting the grid side voltage. When the reference phase angle is locked,  $U_q=0$ , and then equation (1) is further converted into equation (2), thereby realizing the PQ decoupling control of the inverter.

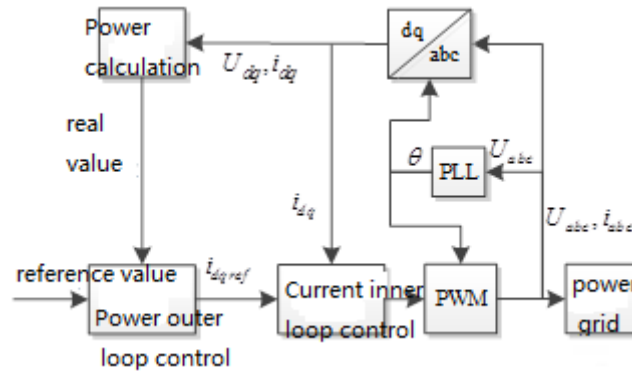


Fig. 1 Frame of double-loop current control.

$$\begin{cases} P = U_d \times i_d + U_q \times i_q \\ Q = -U_d \times i_q + U_q \times i_d \end{cases} \quad (1)$$

$$\begin{cases} P = U_d \times i_d \\ Q = -U_d \times i_q \end{cases} \quad (2)$$

In FIG. 1, the power outer loop module performs PI no difference control on the current actual amount based on the reference quantity, and the output quantity  $i_{dqref}$  is used as the current inner loop control reference value. The current inner loop will make the difference between the reference value and the actual value  $i_{dq}$  through the PI link, and the PWM control reference value can be obtained. Therefore, by controlling the reference values of the d-axis current and the q-axis current respectively, it is convenient to flexibly control the active power output and the reactive power output of the inverter. Due to the self-current inner loop control link in the PWM inverter in the DIGSILENT software, only the modeling of the power outer loop control needs to be completed during modeling.

## 2.2 PQ Control Modeling

The IBDG in the grid-connected state generally uses constant power (PQ) control. From the previous section analysis, through dq decoupling, according to equation (2), the constant reference power values  $P_{ref}$  and  $Q_{ref}$  are used as the input reference quantities of the outer loop power control module, combined with the current power actual values  $P$ ,  $Q$  for PI no difference control. , output a constant current inner loop reference value. Design the inverter PQ control frame in DIGSILENT as shown in Figure 2.

The phase-locked loop PLL provides the phase reference  $\cos\theta$  and  $\sin\theta$  to ensure that the output phase of the distributed power inverter is synchronized with the grid side; PQmea is the power measurement module, which provides the actual active  $p_{in}$  and reactive  $q_{in}$  for the PQ control link; PQ\_control is PQ The control module is controlled by the power outer loop, and the content of the specific control module is shown in FIG. 3 . In FIG. 3, the PQ\_control module receives the actual output active power  $p_{in}$  and reactive power  $q_{in}$  collected by the measurement module, and is different from the set active power reference value  $p_{ref}$  and the reactive power reference value  $q_{ref}$ , and the obtained result passes through the PI control link. And the limiting link, after eliminating the control error, output constant  $i_{d\_ref}$  and  $i_{q\_ref}$  as the reference value of the inverter PWM control current inner loop control.

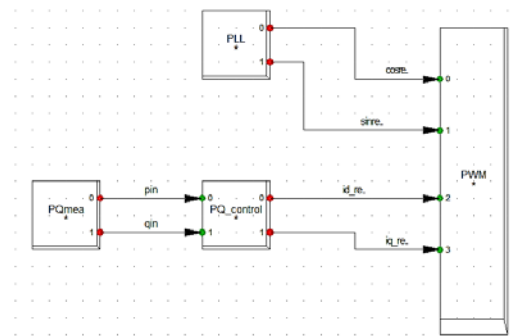


Fig. 2 Frame of IBDG under PQ control.

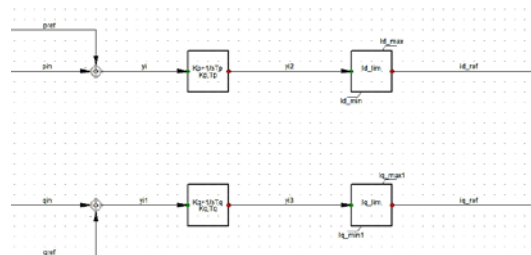


Fig. 3 PQ control.

### 2.3 V/f control modeling

When the microgrid enters the island operation, due to the loss of the FM unit, the distributed power supply in the microgrid is required to operate as a new equilibrium node. At this time, in order to satisfy the frequency and voltage stability of the island operation, the IBDG needs to enter the constant voltage constant

frequency (V/f) control mode. The V/f control is based on the drooping characteristics of the IBDG, and achieves the purpose of controlling the frequency and voltage stability by controlling the active power and reactive power output from the inverter.

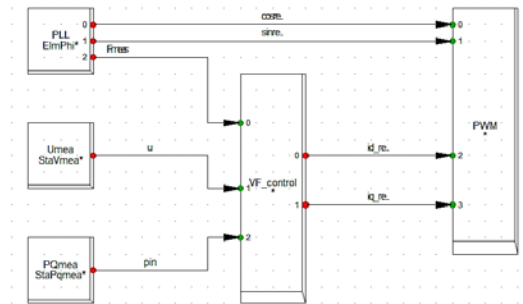


Fig. 4 Frame of IBDG under V/f control.

The V/f control frame of the inverter is shown in Figure 4. The phase-locked loop PLL provides the phase reference values  $\cos\theta$  and  $\sin\theta$  for the inverter control on the one hand, and the current grid-side frequency actual value  $F_{meas}$  for the VF\_control module on the other hand; the power measurement module and the voltage measurement module are respectively PQmea and Umea; For the VF\_control module, the current actual inverter active output  $p_{in}$  and the IBDG terminal voltage  $u$  are provided; the VF\_control module is a V/f controlled outer loop power control module, which is the key to realizing the constant voltage constant frequency in the island, and its specific model is shown in FIG. 5.

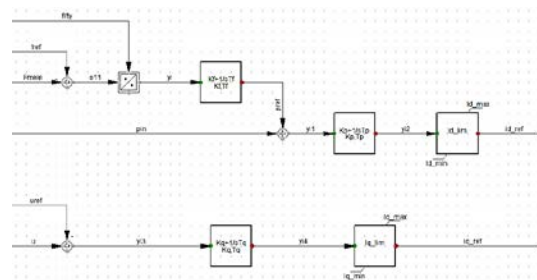


Fig. 5 V/f control.

The constant frequency control of the VF-control module is realized by d-axis control. In Figure 5, the d-axis consists of two links. The first is the frequency link. First, the actual system frequency  $F_{meas}$  is compared with the reference frequency  $f_{ref}$  (power frequency 50Hz). The difference is obtained by the PI link to obtain the active power reference value  $p_{ref}$ . The input of the control link; in the active control

link, the active power reference value  $p_{ref}$  obtained by the frequency control is compared with the current actual active  $p_{in}$  calculated by the measurement module, and then the d-axis current inner loop is output through the PI link and the limit link. Control baseThe historical record value  $i_{d\_ref}$  achieves the purpose of frequency control by active P.

The constant voltage control of the VF-control module is realized by q-axis control. In FIG. 5, the actual IBDG terminal voltage value  $u$  input by the Umea measurement mode is compared with the set reference voltage  $u_{ref}$ , and the obtained difference is outputted through the PI link and the limit link, and the q-axis current inner loop control reference is output. The value  $i_{q\_ref}$  achieves the purpose of voltage control by reactive power Q.

### 3. Failure simulation analysis

A 10kV microgrid with distributed power supply is built in the DIgSILENT simulation software, as shown in Figure 6. Among them, two inverter-type distributed power sources IBDG1 and IBDG2 are respectively obtained by a DC constant voltage source connected to a PWM inverter, and are respectively connected to Bus1 and Bus3 through a 0.4kV/10kV step-up transformer. There are three loads in the microgrid, namely Load 1 on Bus 1, Load 2 on Bus 2, and Load 3 on Bus3. Bus1 and Bus2 are connected by line Line1, and Bus2 and Bus3 are connected by line Line2. Bus 1 is connected upstream to an infinite Grid (Power Grid) as the external grid of the microgrid. When the microgrid is connected to the grid, the External Grid is a balanced node, and both IBDG1 and IBDG2 operate at a constant power with PQ. When the switch between Bus 1 and the infinite power supply is disconnected, the microgrid enters the island operation, and IBDG2 is switched from PQ control to V/f control as the balance node of the three loads and IBDG1. The specific parameters of the grid are as follows: the voltage level on the AC side of the microgrid is 10kV; the voltage on the AC side of the PWM inverter is 0.4KV, and the voltage on the DC side is 0.8kV. Line Line1 has a length of 0.5km and Line2 has a length of 0.2km; line resistance and reactance are 0.797 $\Omega$ /km and 0.105 $\Omega$ /km, respectively. The active power of Load1 is 0.2MW, the reactive power is 0.05Mvar, the active power of Load2 is 0.08MW, the reactive power is 0.02Mvar, the active power of Load3 is 0.1MW, and the reactive power is 0.025Mvar. When connected to the grid, IBDG1 operates at a constant power of 0.1 MW and a reactive power of 0.02 Mvar. IBDG2 operates at a constant power of 0.05 MW and a reactive power of 0.01 MVar.

The control parameters of the PQ\_control module are as follows:  $K_p=1$ ,  $T_p=0.07$ ,  $K_q=1$ ,  $T_q=0.07$ ,  $i_{d\_max}=0.1$ ,  $i_{d\_min}=-0.1$ ,  $i_{q\_max}=0.1$ ,  $i_{q\_min}=-0.1$ .

The control parameters of the VF\_control module are as follows:  $K_f=10$ ,  $T_f=0.004$ ,  $K_p=0.65$ ,  $T_p=0.07$ ,  $K_q=0.65$ ,  $T_q=0.08$ ,  $i_{d\_max}=0.8$ ,  $i_{d\_min}=-0.8$ ,  $i_{q\_max}=0.8$ ,  $i_{q\_min}=-0.8$ .

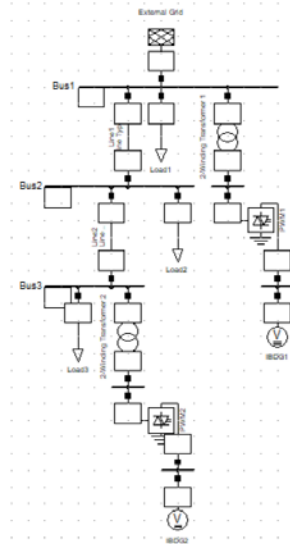


Fig. 6 Microgrid with the interconnection of IBDGs.

### 3.1 Analysis of IBDG fault characteristics when connected to the grid

As shown in Figure 6, in the grid-connected state, at the 1s time, the AB phase-to-phase short circuit fault occurs in the middle of the line Line2 (50%), and the active output, reactive power output, inverter current and terminal voltage of IBDG1 and IBDG2 are at this moment. The change is shown in Figure 7. Since IBDG1 is at the upstream position of the fault point, it has a smaller capacity than the external grid, and almost no short-circuit current is provided. The terminal voltage and its output power change basically. Can be ignored. For the IBDG2 downstream of the fault point, its current output increases significantly at the time of failure, but the voltage at the inverter terminal is significantly reduced. As the voltage at the inverter terminal decreases, both the active output and the reactive output of the IBDG2 are greatly reduced at the time of failure. In addition, although the limiting section is set in the inverter model, since the terminal voltage drops too fast, the short-circuit current output will still exceed the limit.

Figure 8 provides the transient change of the three-phase current at the two ends of the Line2 line at the short-circuit time (1s) with or without IBDG2 access. During normal operation, due to the power compensation of IBDG2, the current flowing through Line 2 when accessing IBDG2 is less than that without access to IBDG2. At the time of failure, because of the two-phase short circuit of AB, there is no significant change in the C-phase current in both cases, and the short-circuit currents of phase A and phase B increase sharply. Compared with the case without IBDG2, when IBDG2 is connected, the short-circuit current downstream (line j) of Line2 increases significantly, while the short-circuit current of upstream (i terminal) of Line2 does not change much, indicating that the short-circuit current provided by

upstream IBDG1 is very short when the line is short-circuited. Limited, but downstream IBDG2 provides significant short-circuit current to Line2. In particular, the C-phase current has also increased significantly after the AB two-phase short circuit. Therefore, the access of the IBDG may cause the traditional three-stage overcurrent protection to malfunction in the downstream. It is worth noting that in Figure 8, when the IBDG2 is connected and the line Line2 is short-circuited by the AB phase, the phase of the phase current at both ends changes in the two phases of the AB. In normal operation, the ABC phase currents at both ends of the Line2 line are opposite in phase (one end is inflow; the other end is out). After the fault, the phase of the two-phase current of the two ends of the Line2 line is changed from the opposite to the opposite; the phase of the C-phase current at both ends of the Line2 line remains opposite. In contrast, the AB phase current across the non-faulty line Line1 in Figure 9 has increased in amplitude after the fault occurred, but the phase remains unchanged. It can be seen that although the access of the IBDG may affect the fault diagnosis of the downstream line, the short-circuit current provided is opposite to the normal operation direction (the phase deviation is close to 180°). Therefore, the fault can be located by phase change of the short-circuit current at both ends of the fault line.

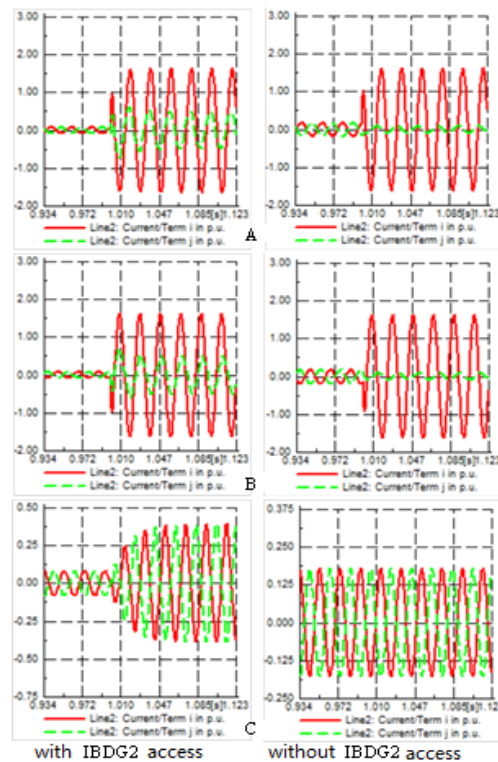


Fig. 8 Influence of interconnection of IBDG2 on short circuit currents at both ends of Line 2 under grid-connected operation.



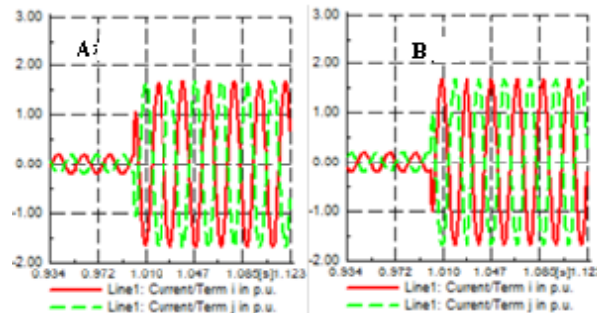


Fig. 9 The phase currents changes of AB phases at both ends of Line 1 when AB interphase fault occurs on Line 2 under grid-connected operation.

In summary, when the IBDG is connected to the grid, its output state is related to whether the terminal voltage is stable. At the fault time, for the IBDG upstream of the fault point, if the connected bus voltage is stable, the output is not greatly affected; for the downstream IBDG of the fault point, since the support voltage of the unbalanced node is stable, both the active output and the reactive output are reduced. However, due to the low voltage of the terminal, its output current is very large, which can provide a considerable short-circuit current, which will affect the downstream protection. From the line side, the phase of the short-circuit current at both ends of the fault line is basically opposite, and the phase of the short-circuit current at both ends of the non-fault line is basically the same.

### 3.2 Analysis of IBDG fault characteristics during isolated islands

When the switch connected to Bus1 and External Grid in Figure 6 is disconnected, the microgrid enters the island operation. IBDG1 is switched from PQ control to V/f control mode. As the island main power source, the frequency and voltage stability in the island are maintained. IBDG2 operates in the same way as when connected to the grid, and still functions as a PQ node with a power of 0.1 MW and a reactive power of 0.025 MW. At the 1s time, the phase-to-phase short-circuit fault occurs in Line 2. The output of IBDG1 and IBDG2 is active, reactive, inverter output current and inverter terminal voltage change at this moment as shown in Fig. 10.

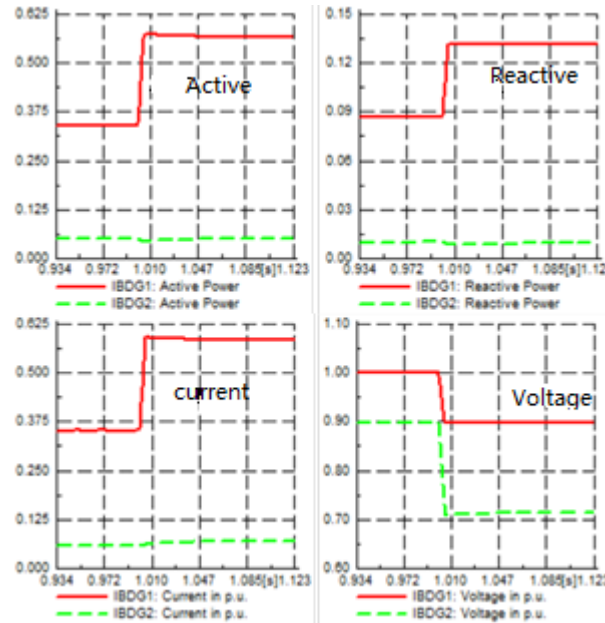
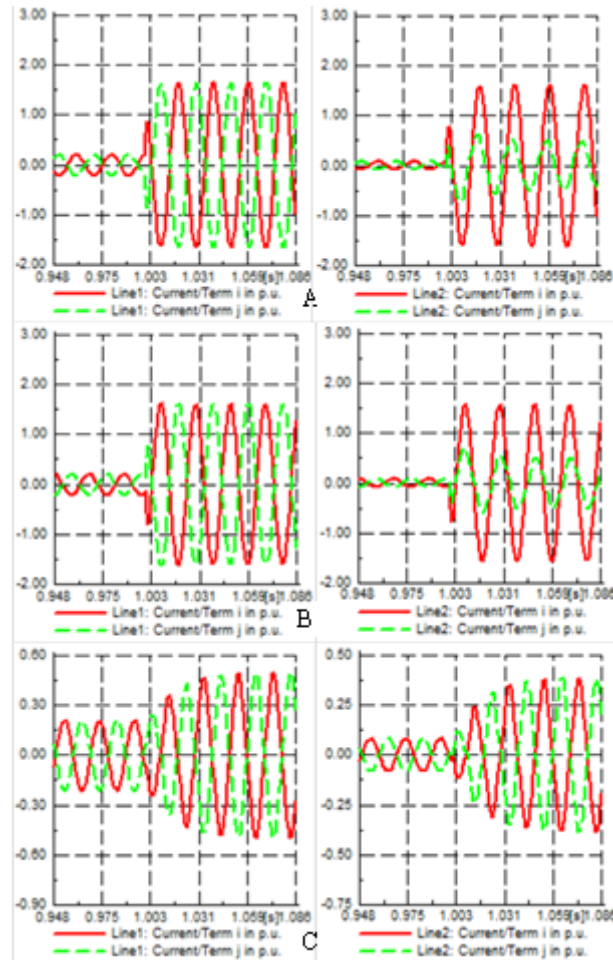


Fig. 10 Fault characteristics of IBDGs under islanding operation.

In Figure 10, since IBDG1 is in constant voltage constant frequency (V/f) control mode, it is equivalent to a balanced node, and the voltage at the IBDG1 inverter terminal remains unchanged after the fault. In order to maintain the terminal voltage and system frequency, the active, reactive, and inverter current outputs of IBDG1 increase sharply, which is more than the short-circuit current provided in the grid-connected state. IBDG2 is now a distributed power supply downstream of the fault point, but it does not provide much short-circuit current. The inverter output current, active power and reactive power have not changed significantly, but the inverter terminal voltage has decreased.

Figure 11 shows the variation of the three-phase currents on the line Line1 and Line2 when the line phase 2 is short-circuited by the AB phase under the island. For line Line1, the AB two-phase current is increased due to the short-circuit current provided by IBDG2. For Line Line2, the AB phase current increases more after the fault than when it is connected to the grid. This is because IBDG1 is no longer a constant power source, but a balanced node. Comparing the changes of the phase of the AB phase current after the fault of the line Line1 and the line Line2, it is found that the phase currents of the two phases of the non-faulty line Line1 remain opposite; and the phase current of the phase line of the faulty line Line2 is about  $180^\circ$ , which is different from the original. The case of IBDG1 access in Figure 8 is similar. Although the IBDG has a limited amplitude link, when it is used as a balanced node, the short-circuit current is higher than that of other IBDGs connected

to the grid, and the characteristics of the current phase deviation at both ends of the faulty line are still applicable to the microgrid system.



*Fig. 11 Three phase currents changes at ends of Line1 and Line2 when AB interphase fault occurs on Line 2 under islanding operation.*

In summary, when the IBDG is in island operation, the IBDG fault characteristics of the PQ control strategy are the same as those in the grid-connected operation; however, the IBDG of the V/f control strategy is larger at the time of failure due to the equilibrium node in the island. The active and reactive outputs also produce a larger short-circuit current than when connected to the grid. From the line side, the phase difference of the short-circuit current at both ends of the fault line is related to the magnitude of the short-circuit current provided by the IBDG downstream of the fault point. Under normal circumstances, the farther the

downstream IBDG is from the fault point, the smaller the short-circuit current is supplied, and the smaller the phase difference is; otherwise, the larger the phase difference is or the opposite.

#### 4. Conclusion

Based on DIgSILENT software, this paper controls the modeling of the inverter distributed power supply (IBDG), which is actually put into operation in the current distribution network, and builds the constant power (PQ) control model and the island state under the grid-connected state. The constant voltage constant frequency (V/f) control model is given, and the specific parameter configuration is given to provide reference for other scholars to carry out DIgSILENT simulation modeling. Based on the built simulation model, the fault simulation was carried out in the grid-connected state and the island state respectively, and the following conclusions were drawn:

(1) When connected to the grid, the short-circuit current provided by the IBDG upstream of the fault point is very limited, and the voltage is relatively stable; and the IBDG downstream of the fault point will provide short-circuit current exceeding the limit even if there is a limiting link. It can be seen that even if there is anti-island protection, the short-circuit current provided by the downstream IBDG in the short-term fault is still large, which easily causes the malfunction of the downstream line protection.

(2) While the island is running, although the short-circuit capacity is smaller than that of the grid-connected operation, the IBDG, which is the main source of the island, will output a larger short-circuit current when the fault occurs, and the IBDG running in the PQ of the island provides a small short-circuit current. The magnitude of the short circuit current is positively related to the distance between the IBDG and the fault point in the microgrid.

(3) From the perspective of fault transients, IBDG has an influence on the current phase difference at both ends of the fault line, but has no effect on the current phase difference at both ends of the non-fault line. Therefore, it can be considered to determine the faulty line by comparing the changes in the phase of the fault current across the line.

(4) From the perspective of fault steady state, IBDG output capacity is limited, and it drops to a relatively low level within a certain period of time after a short-term current increase. If the protection side can escape the transient current influence, the three-stage current Protection is still applicable to distribution systems with IBDG, but processing time will be extended and there will be some damage to the system.

#### References

- [1] Wang Chengshan, Li Peng. Development and Challenges of Distributed Generation, Microgrid and Smart Distribution Network[J]. Automation of

- Electric Power Systems, 2010, 34(2): 10-14.
- [2] WANG C S, LI P. Development and challenges of distributed generation, the micro-grid and smart distribution system [J]. Automation of Electric Power Systems, 2010, 34(2): 10-14.
- [3] Ochoa L F, Harrison G P. Minimizing energy losses: Optimal accommodation and smart operation of renewable distributed generation [J]. IEEE Transactions on Power Systems, 2011, 26(1): 198-205.
- [4] Banerjee B, Islam S M. Reliability based optimum location of distributed generation [J]. International Journal of Electrical Power & Energy Systems, 2011, 33(8): 1470-1478.
- [5] Liu Yanghua, Wu Zhengqiu, Tu Youqing, et al. Overview of distributed generation and its grid-connected technology[J]. Power System Technology, 2008, 32(15): 71-76.
- [6] LIU Y H, WU Z Q, TU Y Q, et al. A Survey on Distributed Generation and Its Networking Technology [J]. Power System Technology, 2008,32(15):71-76.
- [7] Barker PP, De Mello R W. Determining the impact of distributed generation on power systems. I. Radial distribution systems [C]//Power Engineering Society Summer Meeting, 2000. IEEE. IEEE, 2000, 3: 1645-1656 .
- [8] Zhang L, Sidhu T S. New Dynamic Voltage and Reactive Power Control Method for Distribution Networks with DG Integration [C]//Electrical Power and Energy Conference (EPEC), 2014 IEEE. IEEE, 2014: 190-195.
- [9] Pouresmaeil E, Mehrasa M, Catalão J P S. A multifunction control strategy for the stable operation of DG units in smart grids [J]. IEEE Transactions on Smart Grid, 2015, 6(2): 598-607.
- [10] Pan Guoqing, Zeng Dehui, Wang Gang, et al. Failure Analysis Method of Distribution Network with PQ Control Inverter Distributed Power Supply[J]. Proceedings of the CSEE, 2014, 34(4): 555-561.
- [11] PAN G Q, ZENG D H, WANG G, et al. Fault analysis on distribution network with inverter interfaced distributed generations based on PQ control strategy [J]. Proceedings of the CSEE, 2014, 34(4): 555-561.
- [12] KONG Xiangping, ZHANG Zhe, YIN Xianggen, et al. Study on fault current characteristics and fault analysis method of grid with inverter type distributed power supply[J]. Proceedings of the CSEE, 2013, 33(34): 65-74.
- [13] KONG X P, ZHANG Z, YIN X G, et al. Study on fault current characteristics and fault analysis method of power grid with inverter interfaced distributed generation [J]. Proceedings of the CSEE, 2013, 33(34): 65-74.
- [14] Pan Tinglong, Wan Hongshu, Ji Zhicheng. Research on the operation of microgrid island based on improved droop control[J]. Control Engineering, 2014, 21(4): 496-500.
- [15] PAN T L, WAN H J, JI Z C. Research on islanded operation of microgrids based on improved droop control [J]. Control Engineering of China, 2014, 21(4): 496-500.
- [16] Caldon R, Stocco A, Turri R. Feasibility of adaptive intentional islanding operation of electric utility systems with distributed generation [J]. Electric Power Systems Research, 2008, 78(12): 2017-2023.
- [17] WU Ning, XU Yang, LU Yuping. A New Algorithm for Fault Segment

- Location of Distribution Network under Distributed Generation[J]. Automation of Electric Power Systems, 2009 (14): 77-82.
- [18] WU N, XU Y, LU Y P. New fault section location algorithm for distribution network with DG[J]. Automation of Electric Power Systems, 2009 (14): 77-82.
- [19] LI Kaiwen, YUAN Rongxiang, DENG Xiangtian, et al. Improved matrix algorithm for ring network fault location with distributed power supply[J]. Electric Power System and Automation, 2014, 26(12): 62-68.
- [20] LI K W, YUAN R X, DENG X T, et al. Improved matrix algorithm for fault location in ring distribution system with distributed generations [J]. Proceedings of the CSU-EPSA, 2014, 26(12): 62-68.